Am J Physiol Renal Physiol 304: F1428–F1437, 2013.
First published April 3, 2013; doi:10.1152/ajprenal.00444.2012.

βENaC is required for whole cell mechanically gated currents in renal vascular smooth muscle cells

Wen-Shuo Chung,[1] Jennifer L. Weissman,[1] Jerry Farley,[2] and Heather A. Drummond[1]

[1]*Department of Physiology and Biophysics and the Center for Excellence in Cardiovascular-Renal Research, University of Mississippi Medical Center, Jackson, Mississippi; and* [2]*Department of Pharmacology and Toxicology, University of Mississippi Medical Center, Jackson, Mississippi*

Submitted 6 August 2012; accepted in final form 1 April 2013

Chung WS, Weissman JL, Farley J, Drummond HA. βENaC is required for whole cell mechanically gated currents in renal vascular smooth muscle cells. *Am J Physiol Renal Physiol* 304: F1428–F1437, 2013. First published April 3, 2013; doi:10.1152/ajprenal.00444.2012.—Myogenic constrictor responses in small renal arteries and afferent arterioles are suppressed in mice with reduced levels of β-epithelial Na^+ channel (βENaC$^{m/m}$). The underlying mechanism is unclear. Decreased activity of voltage-gated calcium channels (VGCC) or mechanically gated ion channels and increased activity of large conductance calcium-activated potassium (BK) channels are a few possible mechanisms. The purpose of this study was to determine if VGCC, BK, or mechanically gated ion channel activity was altered in renal vascular smooth muscle cell (VSMC) from βENaC$^{m/m}$ mice. To address this, we used whole cell patch-clamp electrophysiological approaches in freshly isolated renal VSMCs. Compared with βENaC$^{+/+}$ controls, the current-voltage relationships for VGCC and BK activity are similar in βENaC$^{m/m}$ mice. These findings suggest neither VGCC nor BK channel dysfunction accounts for reduced myogenic constriction in βENaC$^{m/m}$ mice. We then examined mechanically gated currents using a novel in vitro assay where VSMCs are mechanically activated by stretching an underlying elastomer. We found the mechanically gated currents, predominantly carried by Na^+, are observed with less frequency (87 vs. 43%) and have smaller magnitude (-54.1 ± 12.5 vs. -20.9 ± 4.9 pA) in renal VSMCs from βENaC$^{m/m}$ mice. Residual currents are expected in this model since VSMC βENaC expression is reduced by 50%. These findings suggest βENaC is required for normal mechanically gated currents in renal VSMCs and their disruption may account for the reduced myogenic constriction in the βENaC$^{m/m}$ model. Our findings are consistent with the role of βENaC as a VSMC mechanosensor and function of evolutionarily related nematode degenerin proteins.

epithelial Na^+ channel; ion channel; degenerin; myogenic constriction

THE MYOGENIC RESPONSE IS AN inherent property of small arteries and arterioles in certain organs, including the kidney. The myogenic response is characterized by vasoconstriction following an increase in intraluminal pressure and vasodilation following a decrease in intraluminal pressure. Myogenic constriction is a physiologically relevant response. In the kidney, it is an important mechanism of renal autoregulation, critical for maintaining normal renal blood flow and glomerular filtration rate with changes in perfusion pressure. Recent studies also suggest myogenic constriction plays an important role in protecting against pressure-related renal injury by preventing transmission of systemic pressure swings to delicate renal microvasculature (28, 29, 42).

There are at least three ion channels that play important roles in the myogenic response; mechanically gated ion channels, voltage-gated calcium channels (VGCC), and large conductance calcium activated potassium (BK) channels. The current understanding is that intravascular pressure induces a longitudinal stretch of vascular smooth muscle cells (VSMCs) that are circumferentially arranged in the vessel wall. VSMC stretch is thought to activate a "mechanosensor" of unknown identity (7, 19, 21). Although multiple candidates have been suggested, mechanosensitive ion channels tend to be favored. Activation of the "mechanosensor" leads to Na^+ or Ca^{2+} entry and membrane depolarization, with subsequent activation of VGCC. Activation of VGCC leads to Ca^{2+} entry and vasoconstriction (7, 19). BK channels have also been proposed to participate in myogenic constriction (7, 9, 16, 20). On one hand, they serve an inhibitory role: in response to the large influx of Ca^{2+}, BK channels are activated and prevent excessive vasoconstriction. On the other hand, inhibition of BK channels has been shown to enhance the myogenic response. Furthermore, enhanced BK activity is thought to be an underlying mechanism for the loss of myogenic constriction in certain genetic models (41, 42). Thus inhibition of mechanosensitive ion channels or VGCCs and excessive activation BK channels could inhibit myogenic response.

Our laboratory has hypothesized that vascular degenerin proteins may form the mechanosensitive ion channels in VSMCs that mediate the renal myogenic response. Degenerin proteins are a large family of proteins with a strong evolutionary link to mechanotransduction. Members of this family form ion channels in nematodes that are required for mechanosensory responses. Recently, our laboratory has demonstrated that at least one degenerin protein, β-epithelial Na^+ channel (βENaC), is required for renal myogenic regulation in vitro and in vivo (15, 18, 23). We have identified a mouse model with reduced levels of βENaC in renal VSMCs (βENaC$^{m/m}$). In this model, myogenic regulation of renal afferent arterioles and small arteries is inhibited. However, the mechanism(s) underlying the loss of myogenic constriction in βENaC$^{m/m}$ model is unclear. The purpose of this investigation was to determine if VGCC, BK, and/or mechanically gated ion channels are altered in this model. Our findings demonstrate that VGCC and BK currents activities are not significantly changed in renal VSMCs from βENaC$^{m/m}$ mice and are unlikely to account for the loss of renal myogenic constriction observed in βENaC$^{m/m}$ mice. Moreover, we found that mechanically gated currents are reduced in occurrence and magnitude in renal VSMCs from βENaC$^{m/m}$ mice. Thus our findings suggest that

Address for reprint requests and other correspondence: H. A. Drummond, Dept. of Physiology and Biophysics, Univ. of Mississippi Medical Center, 2500 North State St., Jackson, MS 39216-4505 (e-mail: hdrummond@umc.edu).

 1931-857X/13 Copyright © 2013 the American Physiological Society

βENaC is required for normal mechanically gated currents in renal VSMCs.

METHODS

All protocols and procedures described were reviewed and approved by the Institutional Animal Care and Use Committee of the University of Mississippi Medical Center. Studies were conducted in genetically modified mice. Heterozygote $\beta ENaC^{+/m}$ mating pairs on a mixed genetic background were generously provided by E. Hummler and B. Rossier (University of Lausanne, Lausanne, Switzerland). Animals were provided standard rodent chow containing 0.4% Na^+ (Teklad) and water ad libitum. Offspring of heterozygote mating pairs were genotyped at 3 wk of age using DNA isolated (DirectTail PCR; Viagen) from tail samples and reconfirmed following phenotypic analysis using liver samples as previously described (43). The University of Mississippi Medical Center's Institutional Animal Care and Use Committee approved all animal protocols. Animals were exposed to 12-h light (0600–1800)-dark (1800–0600) cycles.

Preparation of VSMCs. Mice (+/+, 19.5 ± 0.7, n = 44; m/m, 21.8 ± 0.9 wk, n = 20) were anesthetized with isofluorane, and the kidneys were removed. Kidneys were hemisected, decapsulated, and then gently pressed against a 106-μm mesh sieve using the plunger of a glass 30-cc syringe and rinsed with low external Ca^{2+} solution [(in mM) 140 NaCl, 5 KCl, 0.15 $CaCl_2$, 1 $MgCl_2$, 10 HEPES, and 5.5 D-glucose, pH 7.4]. Renal vessels were dissected from adjacent tissue and collected into iced low external Ca^{2+} solution. Tubular cells and connective tissue were further removed from the collected vascular trees by digestion at room temperature first in a low Ca^{2+} enzyme solution containing protease type XIV (1 mg/ml; Sigma-Aldrich, St. Louis, MO) for 5 min, followed by another 5 min in solution containing protease type XIV (1 mg/ml) plus collagenase type IV (2 mg/ml; Worthington). The partially digested vessels were finally incubated with collagenase type IV (2 mg/ml) alone at room temperature for 5 min. After removal of the enzyme, the digested vessels were stored at 4°C. Single renal VSMCs were released by trituration immediately before plating. Cells are plated on collagen and elastomer-coated coverslips and incubated at 4°C for 15–20 min, followed by 15–20 min at room temperature before assessment of currents.

Patch-clamp electrophysiology. Whole cell currents were recorded using conventional patch-clamp techniques with an Axopatch 200B amplifier (Axon Instruments) interfaced to a PC through Digidata1440A digitizer (Axon Instruments) as previously described (4, 5). Data were sampled at 5 kHz and filtered at 1 kHz using a low-pass Bessel filter. pCLAMP10.0 (Axon Instruments) was used for data acquisition. Patch pipettes were pulled from borosilicate filamentous glass capillaries (G150TF-4; Warner Instruments) using a Model P-87 micropipette puller (Sutter Instrument) and polished using a MF-830 Microforge (Narishige). The resistances of patch pipettes used ranged from 6 to 12 MΩ. Fast capacitance transients were compensated before forming the whole cell configuration. Series resistances were below 30 MΩ and were not compensated.

Cells were maintained in low external Ca^{2+} solution, except where noted. Command voltage for continuous recording in the voltage-clamp mode was −40 mV. The pipette (internal) solution was designed to create a Cl^- Nernst potential (E_{Cl}) near the command voltage to minimize the interference from the spontaneous activity of Ca^{2+}-activated Cl^- currents, which contained (in mM) 97 K-gluconate, 27 KCl, 3 NaCl, 1 $MgCl_2$, 20 HEPES, and 0.1 EGTA, 4 ATP-Na_2, and 0.05 GTP-Tris, pH 7.2.

Measurement of VGCC and BK activity. For assessment of VGCC and BK, VSMCs were plated on 25-mm glass coverslips. For the determination of the current-voltage (*I-V*) relationship for the VGCC activation profile, a voltage-step protocol was used, where currents were activated by 1-s voltage steps from a holding potential of −80 mV every 15 s, and the maximum current was obtained for each voltage step from −80 to +60 mV in 10 mV increments. The external solution was replaced with Ba^{2+} solution containing (in mM) 140 tetraethyl-ammonium Cl, 20 $BaCl_2$, 1 $MgCl_2$, 5 4-aminopyrodine, 10 HEPES, and 5.5 D-glucose, pH 7.4. The internal solution used contained (in mM) 135 CsCl, 10 HEPES, 2 EGTA, 4 ATP-Mg, and 0.25 GTP-Tris, pH 7.2.

For the evaluation of BK channel activity, an *I-V* relation was determined by obtaining a mean steady-state current for each tested voltage steps ranging from −80 to +120 mV in 20-mV increments. The pipette solution is designed to clamp internal free [Ca^{2+}] at 100 nM, which contained (in mM) 97 K-gluconate, 23 KCl, 3 NaCl, 1 $MgCl_2$, 2 $CaCl_2$, 20 HEPES, and 5.19 EGTA, 4 ATP-Na_2, and 0.05 GTP-Tris, pH 7.2.

Measurement of mechanically gated currents. For assessment of mechanically gated currents, our laboratory modified a previously used approach (3, 24, 26) in which cells are plated on a flexible elastomeric membrane coated coverslip. The elastomeric membrane was prepared by coating coverslips (25 mm) with 350 μl of Sylgard 184 (Dow Corning; base:curing agent = 30:1) cured at 90°C for 1.5h. To create a hydrophilic surface, cured elastomer-coated coverslips were then treated with a "piranha solution," a mixture of sulphuric acid (H_2SO_4, 98% GR) and hydrogen peroxide (H_2O_2, 30% purified) at 3:2, for 15 min followed by a dip in 2 N KOH for another 15 min before wash-off with distilled water (30). The treated surfaces were then coated with collagen I solution (200 μl, 0.01% collagen I; Sigma) and allowed to adhere and dry at 4°C overnight. Prepared coverslips were stored at 4°C until use.

To assess mechanically gated currents, VSMCs with an elongated shape with clear borders, suggesting adherence to the substrate, were selected. Cells that remained attached to the substrate after withdrawal of the patch pipette at the end of the experiment were considered sufficiently adherent and used for analysis. Through each experiment, we monitored the seal and access resistance of each patch. An experiment would be terminated whenever the membrane resistance dropped below 1 GΩ, or access resistance rose above 30 MΩ to exclude the possibility that the currents elicited using this setting were due to leakage of the seal. The system used to mechanically activate the VSMCs is shown in Fig. 1*A*. The mechanical setup is designed to produce fast bilateral stretching on the collagen-coated elastomer, where cells are plated (Fig. 1*A*). The microrobotic stretching arms are pneumatically driven, capable of movement ranging from 10 to 100 μm within 100 ms, and consistently produce movement in proportion to the driving pressure in the tested range while engaged on the elastomer (Fig. 1, *B* and *C*; n = 6, tested on 2 different preparations of elastomer, 3 different spots from each). Pneumatic pressure pulse is generated by a pressure control unit and delivered to the microrobot through polyethylene tubing. The pressure control unit contains a pressure generator (pipette perfusion pressure/vacuum generator by ALA Scientific Instruments) and programmable solenoid valves (DAD-12 superfusion system by ALA Scientific Instruments). By programming the opening of solenoid valves, we can precisely generate near-square pulse of stretching of the same duration. Plated VSMCs were oriented longitudinally in between the microrobotic stretching arms (~400 μm apart). The microrobotic stretching arms are pressed ~3 μm into the elastomeric surface. A pressure pulse of air controlled by the solenoid valves drives the microrobotic arms out and away from the central zone (Fig. 1*B*) and creates a uniform bilateral stretch of the substrate and overlying adherent VSMCs.

Na^+ selectivity. To determine if Na^+ is the major charge carrier of the mechanically gated currents, we assessed *1*) the *I-V* relationship and reversal potential before and during stretch using a voltage-ramp protocol with voltage ramping from −80 to +40 mV in 50 ms, and *2*) whole cell mechanically evoked currents before and after replacement of external Na^+ with equimolar *N*-methyl-D-glucamine ($NMDG^+$).

Dose (mechanical stimulus)-response (inward peak amplitude) curve. To obtain the relationship between the magnitude of mechanical stimulus and the amplitude of mechanically gated current, cells were subjected to a series of 1-s stretches of the underlying elastomer,

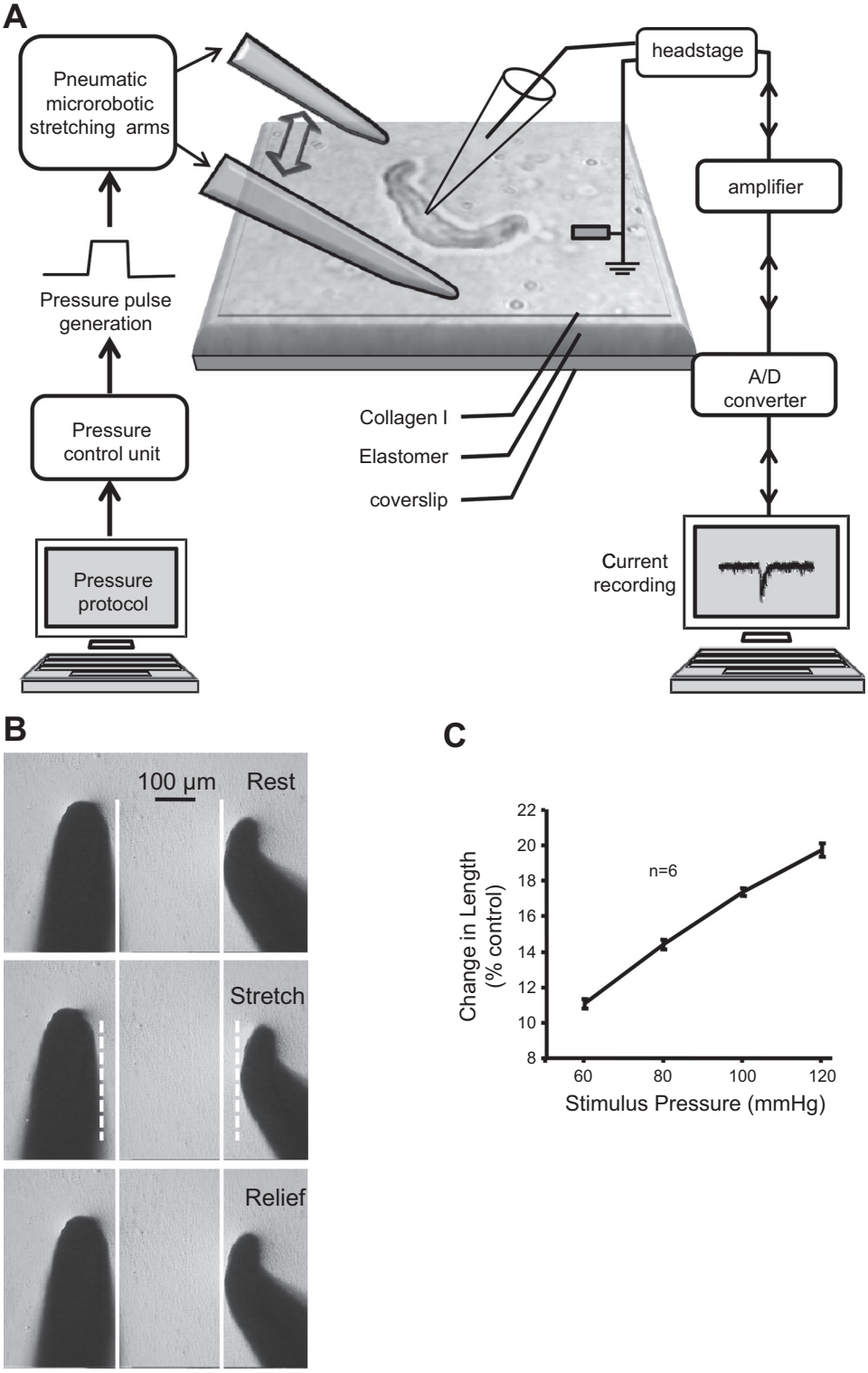

Fig. 1. Measurement of mechanically gated currents. *A*: preparation schematic. Vascular smooth muscle cell (VSMCs) are plated onto collagen I-coated elastomeric membranes. A VSMC is oriented longitudinally between 2 stretching arms and configured with a whole cell patch. A computer-controlled pressure generator generates a pressure pulse to drive the microrobotic stretching arms out and away from the VSMC poles. Elastomer stretch, in turn, stretches the overlaying VSMC. *B*: series of pictures of the stretching arms at baseline (*top*), during stretch (*middle*), and following recovery (*bottom*) from stretch. Note that the 2 arms move an equal distance in the opposite direction and return to their original position following release. Solid white lines identify the location of the stretching arms at *top*. Dashed white lines identify the position of the stretching arms during stretch. *C*: mean relationship between the driving pressure and elastomer stretch. This graph demonstrates the increases in driving pressure produce proportional increases in elastomer stretch and is highly repeatable among samples. Substrate length increases ~11% at 60 mmHg and ~20% at 120 mmHg.

with driving pressure for the stretching arms stepping from 60 to 140 mmHg, in 20-mmHg increments, 2–3 min apart. The peak current amplitude for each stretch was plotted against the driving pressure as an index for the magnitude of mechanical stimulus exerted on the underlying substrate. Current amplitude was not plotted as a function of cell length because preliminary studies suggested VSMCs with a slight crescent shape were more likely to respond to stretch and the curvature complicated a determination of length change along the longitudinal axis.

Data analysis. Patch-clamp data were analyzed offline using Clampfit 10 (Axon Instruments). All data are presented as means ± SE, where *n* is the number of cells examined. Data were compared using paired *t*-test, ANOVA, repeated-measures ANOVA, or two-way ANOVA on ranks with Student-Newman-Keuls post hoc test where

appropriate. Statistical difference was considered significant at $P < 0.05$.

RESULTS

VGCC and BK current activities in renal VSMCs from βENaC$^{+/+}$ vs. βENaC$^{m/m}$ mice. To determine if the impaired myogenic response observed in βENaC$^{m/m}$ mice might be attributed to any alteration in its activity of VGCC or BK, we compared the *I-V* relations of VGCC (Fig. 2*A*) and BK (Fig. 2*B*) activity in renal VSMCs from βENaC$^{+/+}$ and βENaC$^{m/m}$ mice. First, we examined VGCC activity in VSMCs from βENaC$^{+/+}$ and βENaC$^{m/m}$ mice. As shown in Fig. 2*A*, the activation profile of VSMC VGCC is similar between βENaC$^{m/m}$ and βENaC$^{+/+}$mice. Both have their maximum activation occur between +10 and +20 mV (Fig. 2*A*; $n = 6$ each). Next, we examined BK activity and observed a rightward shift in the current density vs. voltage relationship in renal VSMCs from βENaC$^{m/m}$ mice (Fig. 2*B*; $n = 6$). Mean BK current density was similar in βENaC$^{m/m}$ and wild-type controls (Fig. 2*B*). These findings suggest that changes in neither BK nor VGCC function mediate the reduced renal myogenic constrictor responsiveness observed in βENaC$^{m/m}$ mice.

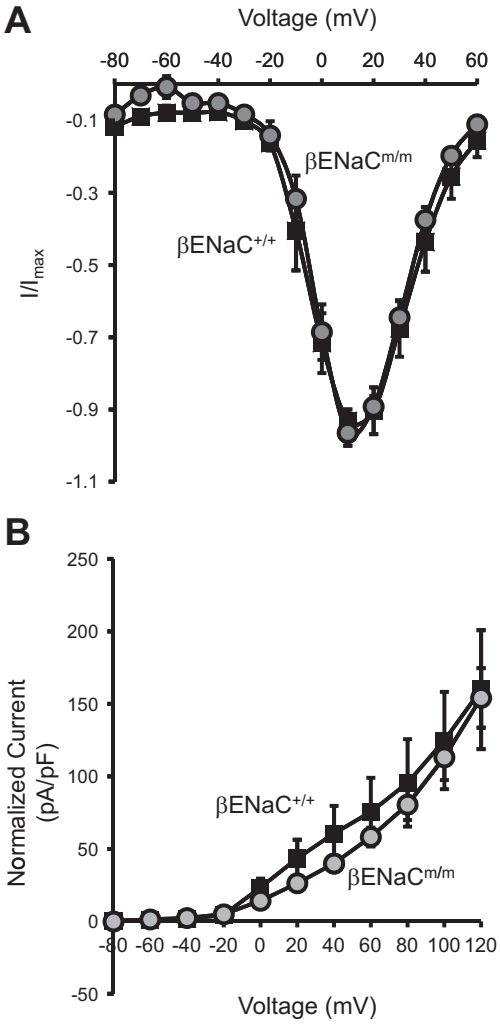

Fig. 2. Voltage-gated calcium channels (VGCC) and large conductance calcium-activated potassium (BK) current activities in renal VSMCs from β-epithelial Na^+ channel (βENaC)$^{+/+}$ vs. βENaC$^{m/m}$. *A*: for VGCC current activity, there is no significant difference in the activation profiles of VGCC in renal VSMCs from βENaC$^{+/+}$ vs. βENaC$^{m/m}$. *I-V* relationships for VGCC were obtained by using Ba^{2+} as a surrogate for Ca^{2+}. Currents were activated by 1-s voltage steps from a holding potential of −80 mV every 15 s from −80 to +60 mV in 10-mV increments. The maximum current from each voltage step was used for plotting the activation *I-V* relationship ($n = 6$ per group). *B*: for BK current activity, *I-V* relationships were determined by a series of voltage steps ranging from −80 to +120 mV in 20-mV increments ($n = 6$ cells per group).

Substrate stretch elicits mechanically gated currents in dissociated renal VSMCs. Several reports suggest the myogenic response is initiated by the activation of mechanosensitive ion channels (6, 7, 19, 21). Since βENaC has strong evolutionary ties to mechanosensing, we wanted to determine if βENaC contributes to mechanically gated currents in renal VSMCs. To address this, our laboratory developed a novel assay to elicit mechanically gated currents in isolated VSMCs. In this assay, VSMCs plated on a collagen-coated elastomeric membrane are mechanically stimulated by stretch of the underlying membrane, which leads to displacement of the VSMC. A representative example of VSMC displacement/stretch and the mechanically gated current is shown in Fig. 3, *A–C* (from βENaC$^{+/+}$). Individual images of a representative VSMC at rest (Fig. 3*A*, *top*), during stretch (*middle*), and following release (*bottom*) are shown with its border outlined. An overlay of the VSMC outlines at rest and during stretch (Fig. 3*B*) indicates a modest displacement of the VSMC poles with elastomer stretch (100-mmHg driving pressure). The mechanically gated whole cell current for the VSMC shown in Fig. 3, *A* and *B* is shown in *C*, *top trace*. The *bottom trace* shows an example of mechanically gated current recorded from another renal VSMC. Both representative traces highlight the same feature of a fast initial transient that quickly tapers off despite the presence of stretch stimulus. The repeatability of the mechanically gated current is shown in Fig. 3*D*. There is no significant change in the current amplitudes within three trials when VSMCs were subjected to repeated stretches at 2- to 3-min intervals ($n = 12$).

VSMC mechanically gated currents are mainly carried by Na^+. The mechanically gated inward currents were recorded in cells voltage clamped at near E_{Cl} (−40 mV), which should exclude the possibility of Cl^- serving as a charge carrier for the currents. Due to the composition of the external solution, the evoked currents are likely to be carried by Na^+. To address this possibility, we used a voltage-ramp protocol to determine if elastomer stretch altered the reversal potential (Fig. 4, *A* and *B*). Figure 4*A*, *left*, shows the mean *I-V* relations before stretch (black solid trace) and during elastomer stretch (gray solid trace); the net effect of stretch on *I-V* relation is shown at *right* (dashed lines give the range of standard error; $n = 7$). There are two findings that favor Na^+ as the charge carrier: *1*) the rightward shift of the reversal potential, and *2*) the larger net inward currents at the more negative voltages. To further evaluate the importance of external Na^+, we compared the stretch-evoked currents in normal (140 mM Na^+) and Na^+-free (with Na^+ replaced by equimolar $NMDG^+$) conditions. A representative trace is shown in Fig. 4*C*, and group data are shown in Fig. 4*D*. These data demonstrate that Na^+ accounts for about 90–95% of the peak and total current evoked during stretch (area under curve; $n = 6$). These findings suggest that Na^+ is the predominant charge carrier of mechanically gated currents in renal VSMCs.

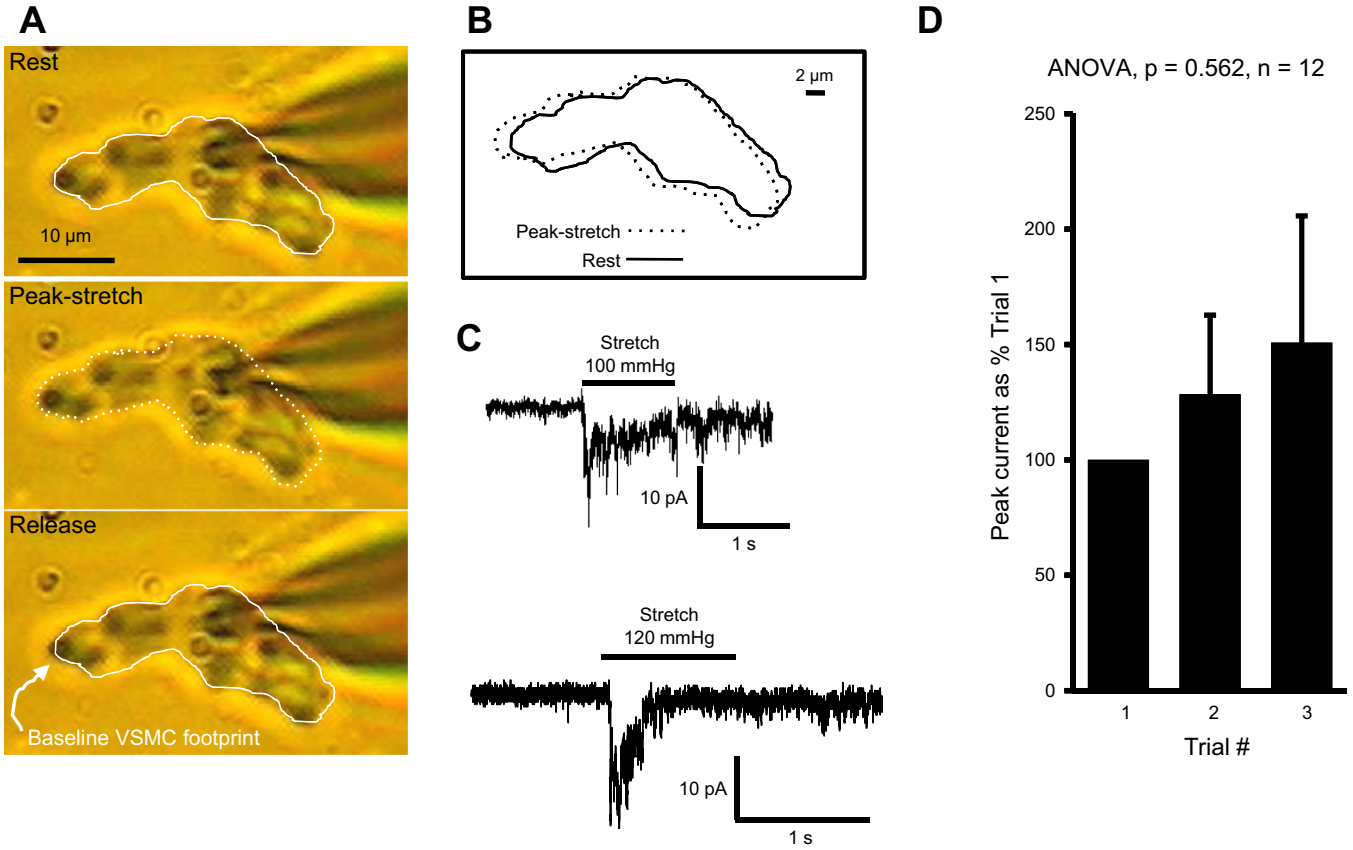

Fig. 3. Mechanically gated currents are activated through stretch of the underlying elastomer. *A*: representative images of a VSMC subjected to elastomer stretch with 100-mmHg driving pressure. VSMC border is outlined at baseline (*top*), during peak-stretch (*middle*), and following recovery (*bottom*). *B*: overlay of the VSMC outlines from baseline and peak stretch shows a modest displacement of the VSMC during elastomer stretch. *C*, *top trace*: mechanically gated current evoked in the same VSMC shown in *A* and *B*. *C*, *bottom trace*: example of mechanically gated current recorded from another renal VSMC. *D*: repeated activation of the mechanically gated current shows no significant change in the amplitude the currents within 3 stimuli (100-mmHg driving pressure) at 2- to 3-min intervals (repeated measures ANOVA; $n = 12$ VSMCs).

Amplitude of stretch-evoked current is decreased in renal VSMCs from βENaC$^{m/m}$ mice. Mechanosensitive ion channels are considered to be at least one mechanism that may initiate the myogenic response (7, 19, 21). Since βENaC is evolutionarily related to presumed mechanically gated channels in the nematode, we speculate that βENaC contributes to the ion-conducting pore of a mechanosensor in VSMCs (10, 11, 40). To test this possibility, we examined mechanically gated currents in renal VSMCs in βENaC$^{+/+}$ and βENaC$^{m/m}$ mice (Fig. 5). We evaluated current responses of VSMCs to stretch of the underlying matrix generated by our pneumatically driven device using step-wise increases in pressure. The mean capacitance was nearly identical in βENaC$^{+/+}$ (12.0 ± 0.5 pF) and βENaC$^{m/m}$ (11.8 ± 0.7) VSMCs. In Fig. 5, *A* and *B*, the amplitudes of the mechanically gated current responses in all βENaC$^{+/+}$ ($n = 53$) and βENaC$^{m/m}$ ($n = 29$) VSMCs are shown as mean peak amplitude (pA; *A*) and normalized to capacitance (pA/pF; *B*). The *P* values for all pair-wise comparisons are provided in Table 1. In βENaC$^{+/+}$ VSMCs, a small inward current is present at the lowest pressure stimuli (60 mmHg) and amplitude increases further at 80 and 100 mmHg and then tends to plateau. In contrast, with increasing pressure stimuli, peak amplitude does not increase significantly in βENaC$^{m/m}$ VSMCs at any driving pressure. At pressure stimuli of 100, 120, and 140 mmHg, the peak amplitude is significantly reduced in βENaC$^{m/m}$ compared with βENaC$^{+/+}$ VSMCs.

After the raw data were examined, there appeared to be two patterns of dose-response relationships: those that had maximum peak current amplitude >15 pA (responders) and those that had none of their peak current amplitudes >15 pA (nonresponders). In Fig. 5, *C* (βENaC$^{+/+}$) and *D* (βENaC$^{m/m}$), the mean amplitudes of the mechanically gated currents in responders and nonresponders are represented by solid and dashed traces, respectively. The *P* values for all pair-wise comparisons are shown in Table 1. In the βENaC$^{+/+}$ VSMCs, 46 out of 53 (87%) VSMCs responded with a peak current >15 pA. In contrast, only 13 out of 29 (43%) VSMCs responded with a peak current >15 pA in the βENaC$^{m/m}$ group. This 50% decrease in the probability of evoking a mechanically gated current >15 pA suggests a remarkably reduced sensitivity to mechanical stimuli in βENaC$^{m/m}$ VSMCs.

Within the βENaC$^{+/+}$ responders group, there is an obvious stimulus dependency of the activated current. There is a small, but significant, increase in current at 80 mmHg, suggesting the threshold for activation may be near the 80-mmHg pressure stimulus. This is followed by a nearly threefold increase in current at 100-mmHg pressure stimulus, which plateaus between 100- and 140-mmHg stimulus pressure. In the βENaC$^{m/m}$ responder group, there is also a small increase in current ampli-

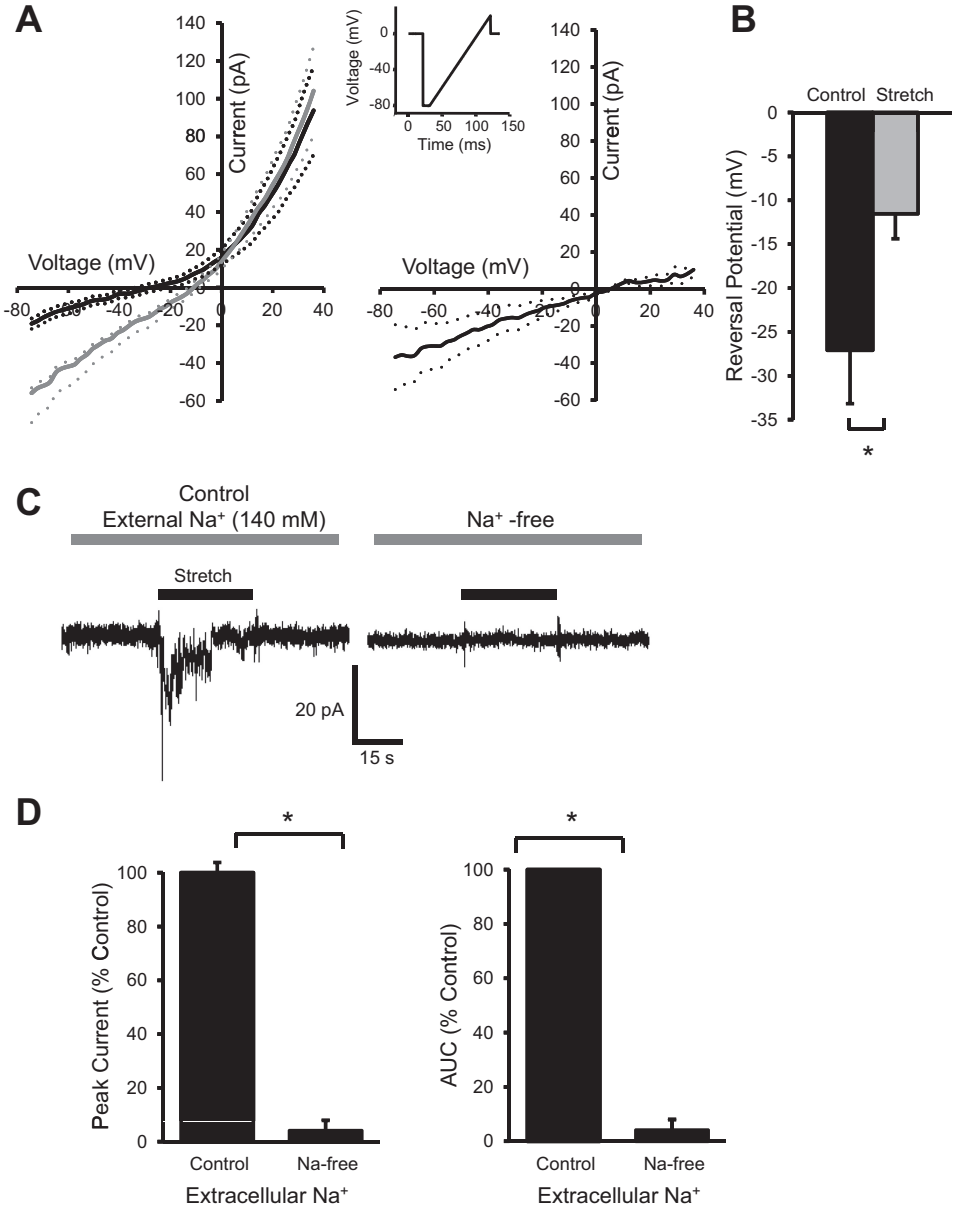

Fig. 4. VSMC mechanically gated currents are mainly carried by Na^+. *A*: an *I-V* relationship was obtained by using a voltage-ramp protocol (*inset*) at baseline (black line, *left*) and during elastomer stretch (gray line, *left*, dashed lines represent the standard errors, $n = 7$). Note the rightward shift of the *I-V* curve with elastomer stretch. *A*, *right*: net effect of elastomer stretch on *I-V* relation obtained by subtracting the current at baseline from current during stretch at each voltage. *B*: reversal potentials of the *I-V* curves shifts towards a more positive potential during stretch, suggesting an increase in conductance for Na^+. *C*, *left*: representative trace at *left* shows a mechanically gated current activated by elastomer stretch under normal external Na^+ concentration (140 mM). *C*, *right*: current trace after the external Na^+ was replaced by equimolar *N*-methyl-D-glucamine ($NMDG^+$). Replacement of Na^+ by impermeant $NMDG^+$ was manifested by the lower basal noise of the trace. *D*: mean peak amplitude (*left*) and total current evoked during elastomer stretch [area under curve (AUC); *right*] of mechanically gated currents were nearly abolished when the external Na^+ was removed ($n = 6$), suggesting Na^+ is the major charge carrier for mechanically gated currents. *Significantly different, $P < 0.05$, paired *t*-test.

tude at 80 mmHg; however, the current does not increase with further increases in stimulus pressure. Taken together, these findings suggest that mechanically gated currents are present in $\beta ENaC^{m/m}$ VSMCs; however, their magnitude and probability are significantly reduced compared with $\beta ENaC^{+/+}$ VSMCs.

DISCUSSION

The myogenic response is an important mechanism of renal autoregulation and protects against pressure-related microvascular injury in kidney. The molecular mechanism underlying the myogenic response is unclear. However, activation of several ion channels has been implicated including BK, VGCC, and mechanically gated ion channels (7, 19, 21). Our laboratory has hypothesized that some mechanically gated ion channels in VSMCs might be formed by vascular degenerin proteins, which might act as mechanosensors because of their strong evolutionary link to mechanosensing in the nematode (10, 11, 40). We have identified a mouse model with reduced levels of βENaC ($\beta ENaC^{m/m}$), in which myogenic regulation of small renal arteries and afferent arterioles is inhibited (15). To further investigate the underlying mechanism of this finding, we determine in the current study if renal VSMC BK, VGCC, or mechanically gated currents are altered in the $\beta ENaC^{m/m}$ model. We found no alteration in VGCC activity in renal VSMCs from $\beta ENaC^{m/m}$ mice. Although we found a modest suppression of BK activity in renal VSMCs from $\beta ENaC^{m/m}$ mice, BK inhibition is not consistent with a loss of renal myogenic constriction. However, we found mechanically gated currents are potently inhibited in renal VSMCs from $\beta ENaC^{m/m}$ mice. These findings suggest βENaC is an important mediator of mechanically gated currents in renal VSMCs and are consistent with the hypothesis that βENaC is a component of vascular mechanosensor.

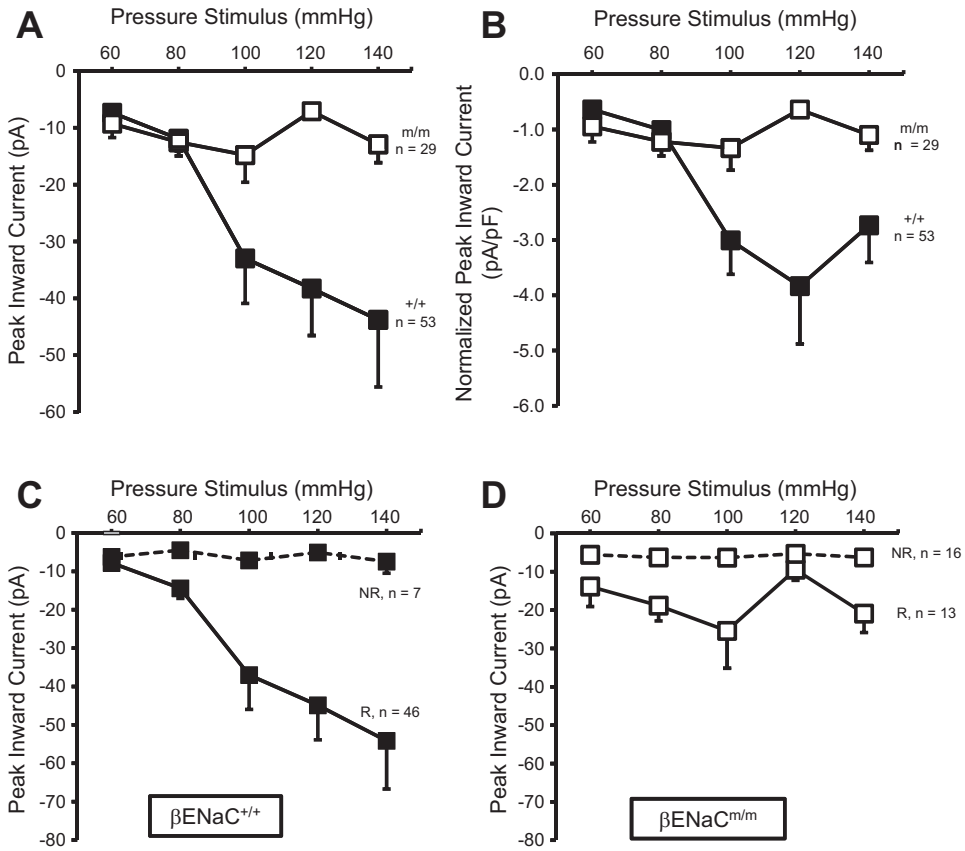

Fig. 5. βENaC contributes to mechanically gated currents in renal VSMCs. *A* and *B*: mean stimulus (driving pressure, 60–140 mmHg)-response (peak current) responses for all renal VSMCs from βENaC$^{+/+}$ (■; n = 53) and βENaC$^{m/m}$ (□; n = 29) mice. Data are presented as mean peak current (pA; *A*) and mean peak current normalized to cell capacitance (pA/pF; *B*). Mechanically gated currents in βENaC$^{+/+}$, but not βENaC$^{m/m}$, VSMCs exhibit a dose-dependent response. *C* and *D*: VSMC responses from βENaC$^{+/+}$ (*C*) and βENaC$^{m/m}$ (*D*) animals were categorized based on whether the maximum peak current amplitude was greater [solid lines, responder (R)] or lesser [dashed lines, nonresponder (NR)] than 15 pA. Mechanically gated currents in VSMCs with maximum peak current amplitude >15 pA had a threshold of 80 mmHg. Mechanically gated current continues to increase with further increases in pressure stimuli greater than 80 mmHg in βENaC$^{+/+}$, but not βENaC$^{m/m}$, VSMCs.

Neither VGCC, nor BK activity, is directly implicated in the impaired renal myogenic constriction in βENaC$^{m/m}$ mice. A broad variety of ion channels have been suggested to be involved in the mechanism of myogenic response (7, 19, 21). Among them, BK and VGCC play important established roles in the regulation of Ca^{2+} influx required for smooth muscle contractility. However, our results indicate that neither VGCC, nor BK, likely account for the impaired myogenic constriction observed in βENaC$^{m/m}$ mice. The activation profile of VGCC and BK currents in renal VSMCs from βENaC$^{m/m}$ mice was very similar to that from their wild-type littermates. Thus our results indicate that neither VGCC, nor BK, likely account for the impaired renal myogenic constriction observed in βENaC$^{m/m}$ model. These findings are consistent with previous findings from our laboratory demonstrating that the contractility of cerebral arteries from βENaC$^{m/m}$ mice is intact in response to high external K^+ concentration, a response dependent on depolarization induced VGCC activation (43).

A mechanoassay that incorporates the extracellular matrix. To determine if mechanically gated currents are altered in the βENaC$^{m/m}$ model, our laboratory adapted a previously published assay (3, 24, 26) for mechanoactivation of isolated VSMCs. Several other assays, such as hypo-osmotic swelling, application of negative pressure to a patched membrane, shear stress, and probing or tugging isolated cells, have been used to mechanically stimulate isolated cells under voltage-clamped conditions (6, 33, 34, 37). However, these approaches are independent of the extracellular matrix, a critical component of the nematode mechanosensor. The nematode mechanosensor model predicts degenerin proteins are tethered to the extracellular matrix and efficient force transduction is dependent on the matrix (12, 14, 27). We hypothesize that βENaC is similarly tethered to the extracellular matrix and requires the matrix for efficient transduction. Therefore, as concerns regarding the lack of extracellular matrix involvement with puffing, stretching, and osmotic swelling assays, we developed this novel mechanoassay. In our mechanoassay, dissociated VSMCs adhered to a collagen-coated elastomeric membrane are stretched bilaterally along their long axis by stretch of the underlying elastomer. We chose collagen I for substrate coating because it is commonly used with VSMCs. Although the currents evoked using our assay suggest an important role of the extracellular matrix in the response, as shown by others, we did not specifically address the type of interaction that may be involved (1, 7, 8, 19, 31, 45).

A limitation of this mechanoassay is the variability; the responses are not highly repeatable within a VSMC. Although the specific reasons underlying this are unclear, we speculate that elastomer stretch may cause a disruption in the cell-matrix contacts, which are reformed during recovery. This breaking and reformation of contacts may account for some of the variability in our signals. Despite this, we have observed an obvious dose dependency of the response (Fig. 5) among VSMCs. We speculate the primary cause of loss of responsiveness is due to breakdown of the interaction between the VSMC and the extracellular matrix, as determined by ruffling/floating/loss of adhesion of VSMC edges from the substrate.

VSMC mechanically gated currents are mainly carried by Na^+. Most degenerin proteins form Na^+ selective channels; however, some also conduct other cations. In our preparation,

Table 1. *P values for all pair-wise comparisons for Fig. 5*

Pressure Stimulus, mmHg	Figure 5, *A–D*			
	A		*B*	
	βENaC$^{+/+}$	βENaC$^{m/m}$	βENaC$^{+/+}$	βENaC$^{m/m}$
Within Genotype Comparison				
60 vs. 80	0.134	0.192	<0.082	0.280
60 vs. 100	<0.001*	0.162	<0.001*	0.325
60 vs. 120	<0.001*	0.748	<0.001*	0.940
60 vs. 140	<0.001*	0.345	<0.001*	0.529
80 vs. 100	0.007*	0.995	0.001*	0.689
80 vs. 120	0.014*	0.383	0.012*	0.548
80 vs. 140	0.017*	0.770	0.041*	0.872
100 vs. 120	0.555	0.214	0.843	0.642
100 vs. 140	0.456	0.957	0.856	0.881
120 vs. 140	0.501	0.520	0.731	0.722
	βENaC$^{+/+}$ vs. βENaC$^{m/m}$		βENaC$^{+/+}$ vs. βENaC$^{m/m}$	
Between Genotype Comparison				
60	0.511		0.617	
80	0.820		0.845	
100	0.007*		0.002*	
120	0.001*		<0.001*	
140	0.013*		0.041*	
	C		*D*	
	βENaC$^{+/+}$		βENaC$^{m/m}$	
	R	NR	R	NR
Genotype Comparison of R vs. NR Within Genotype				
60 vs. 80	0.027*	0.758	0.021*	0.934
60 vs. 100	<0.001*	0.678	0.078	0.934
60 vs. 120	<0.001*	0.708	0.278	0.877
60 vs. 140	<0.001*	0.848	0.042*	0.816
80 vs. 100	0.013*	0.717	0.994	0.807
80 vs. 120	0.002*	0.848	0.273	0.971
80 vs. 140	0.002*	0.845	0.722	0.964
100 vs. 120	0.136	0.770	0.561	0.967
100 vs. 140	0.084	0.816	0.477	0.967
120 vs. 140	0.351	0.870	0.390	0.941
	βENaC$^{+/+}$		βENaC$^{m/m}$	
Comparison of Responders vs. Nonresponders Within Genotype				
60	0.685		0.821	
80	0.004*		0.013*	
100	0.003*		0.051	
120	<0.001*		0.205	
140	0.008*		0.017*	

βENaC, β-epithelial Na^+ channel; R, responders; NR, nonresponders. *Significantly different, $P < 0.05$.

Ca^{2+} is not a likely charge carrier since extracellular Ca^{2+} is low (0.15 mM); thus Na^+, Cl^-, and K^+ are the likely charge carriers. To determine the ion selectivity, we first evaluated the *I-V* relationship in VSMCs before and during stretch and found that substrate stretch caused a rightward shift in the *I-V* curve. Furthermore, the *I-V* curve of the net effect of elastomer stretch crosses the voltage axis at a positive voltage. Since the equilibrium potentials for Na^+, Cl^-, and K^+ are approximately +65, −40, and −80 mV, respectively, in our preparation, the rightward shift of the *I-V* curve with substrate stretch suggests an increase in Na^+ conductance. To confirm the importance of Na^+, we examined mechanically gated currents following removal of extracellular Na^+ and found the mechanically gated inward currents were abolished. Taken together, our findings suggest the mechanically gated currents activated in our mechanoassay may be more selective for Na^+ ions than other cations.

Amplitude of mechanically gated current is dose dependent. A feature of mechano-dependent responses is a graded relationship between the stimulus and the response. We also found an obvious dose-response relationship between pressure stimulus and peak current in renal VSMCs from βENaC$^{+/+}$ mice. Based on the two-way ANOVA on ranks, the first significant increase in current above 60 mmHg is observed at 80 mmHg (Fig. 5*C*) and plateaued between 100 and 140 mmHg. Although several VSMCs within this group clearly had pressure thresholds at 60 or 80 mmHg, several VSMCs did not respond until the 140-mmHg pressure stimulus. This suggests that there is a high level of intersample variability, which may be due to the sensitivity of or our assay or there may be VSMC subpopulations with different response patterns. This would not be unusual since several neuronal mechanoreceptors, such as arterial baroreceptors and tactile receptors, display different response patterns (25, 36).

Amplitude and likelihood of evoking mechanically gated currents is decreased in renal VSMCs from βENaC$^{m/m}$ mice. Previous studies from our laboratory suggest an important role for βENaC in transduction of the myogenic response. However, the importance of βENaC in generation of mechanically gated currents, thought to be the mechanism responsible for initiation of myogenic constriction, has never been addressed. In the current investigation, we demonstrate that mechanically gated currents in renal VSMCs from βENaC$^{m/m}$ mice are *1*) 50% less likely to be evoked, and *2*) 60–70% smaller at the higher stimulus intensities. Therefore, our findings suggest that βENaC is required for normal mechanically gated currents in renal VSMCs. It is important to point out that although our findings demonstrate a requirement for βENaC to elicit the currents, they do not prove that βENaC-containing channels conduct the current. However, based on the crystal structure of the closely related degenerin ASIC1, βENaC is highly likely to contribute to ion permeation (22, 39).

Why is the mechanically gated current not abolished in βENaC$^{m/m}$ VSMCs? It is important to keep in mind that the βENaC$^{m/m}$ model is not a knockout model but rather it is a knockdown model. Several studies indicate βENaC expression is suppressed, but not abolished (15, 35, 43). In a previous study, our laboratory demonstrated VSMC βENaC protein levels, as determined by quantitative immunolabeling, are only inhibited 50% (43). Thus it is highly likely that remaining βENaC could account for the remaining current in βENaC$^{m/m}$ VSMCs. Alternatively, some other degenerins (i.e., ASIC2) or a transient receptor potential (TRP) channel may also account for the current observed in βENaC$^{m/m}$ VSMCs (10, 11). Determining the molecular identity of the mechanically gated current in βENaC$^{m/m}$ VSMCs is beyond the scope of this investigation and will require further study.

Is there a potential role TRP channel proteins? TRP channels are also potential mechanotransducers. Recent studies have shown that inhibition of TRP channels abolishes myogenic vasoconstriction, which has led to the suggestion that TRP channels may act as mechanosensors (13, 33, 38, 44). Indeed, studies in the nematode confirm the importance of TRP channels in mechanotransduction (32). There is little doubt that

both DEG/ENaC and TRP proteins are essential for normal mechanotransduction in VSMCs. However, it is unclear which act as sensors of the mechanical stimuli or participate in the downstream signaling process. A recent study using the nematode model has shed some light on the topic (17). Geffeney et al. (17) elegantly demonstrated that worms with mutations in a degenerin gene (DEG-1) or a TRP gene (TRPV) lack the integrated behavioral responses to stimulation. However, worms with the TRPV mutation have normal mechanoreceptor currents and potential, whereas DEG-1 mutant worms do not. This finding suggests that, at least in this example, the TRP channel is not the sensor of the mechanical stimulus, rather it contributes to a later step in the perception process (i.e., signal transduction/amplification). A similar role may also pertain to other ion channels in myogenic constriction thought to be downstream of TRP channel signaling such as the recently identified role for transmembrane 16a chloride channel (TMEM16a; Ref. 2). Because mammalian VSMCs also appear to coexpress degenerin proteins and TRP proteins, their functions might be evolutionarily conserved. The importance of βENaC and TRP channels as sensors and/or amplifiers in VSMCs remains to be established.

In summary, our findings suggest that the impaired renal myogenic tone observed in $\beta ENaC^{m/m}$ mice is not due to reduced VGCC or enhanced BK. Rather, the impaired renal myogenic tone is likely attributed to a loss of mechanically gated currents, which are primarily carried by Na^+. These findings are consistent with the hypothesis that βENaC, and possibly other vascular degenerin proteins act as mechanosensors in vascular tissue.

GRANTS

This work was supported by the National Heart, Lung, and Blood Institute Grants HL-086996 and HL-51971.

DISCLOSURES

No conflicts of interest, financial or otherwise, are declared by the author(s).

AUTHOR CONTRIBUTIONS

Author contributions: W.-S.C. and J.L.W. performed experiments; W.-S.C. and H.A.D. analyzed data; W.-S.C., J.M.F., and H.A.D. interpreted results of experiments; W.-S.C. and H.A.D. prepared figures; W.-S.C. drafted manuscript; W.-S.C., J.M.F., and H.A.D. edited and revised manuscript; H.A.D. conception and design of research; H.A.D. approved final version of manuscript.

REFERENCES

1. **Balasubramanian L, Ahmed A, Lo CM, Sham JS, Yip KP.** Integrin-mediated mechanotransduction in renal vascular smooth muscle cells: activation of calcium sparks. *Am J Physiol Regul Integr Comp Physiol* 293: R1586–R1594, 2007.
2. **Bulley S, Neeb ZP, Burris SK, Bannister JP, Thomas-Gatewood CM, Jangsangthong W, Jaggar JH.** TMEM16A/ANO1 channels contribute to the myogenic response in cerebral arteries. *Circ Res* 111: 1027–1036, 2012.
3. **Cheng CM, Lin YW, Bellin RM, Steward RL Jr, Cheng YR, LeDuc PR, Chen CC.** Probing localized neural mechanotransduction through surface-modified elastomeric matrices and electrophysiology. *Nat Protoc* 5: 714–724, 2010.
4. **Chung WS, Farley JM, Drummond HA.** ASIC-like currents in freshly isolated cerebral artery smooth muscle cells are inhibited by endogenous oxidase activity. *Cell Physiol Biochem* 27: 129–138, 2011.
5. **Chung WS, Farley JM, Swenson A, Barnard JM, Hamilton G, Chiposi R, Drummond HA.** Extracellular acidosis activates ASIC-like channels in freshly isolated cerebral artery smooth muscle cells. *Am J Physiol Cell Physiol* 298: C1198–C1208, 2010.
6. **Davis MJ, Donovitz JA, Hood JD.** Stretch-activated single-channel and whole cell currents in vascular smooth muscle cells. *Am J Physiol Cell Physiol* 262: C1083–C1088, 1992.
7. **Davis MJ, Hill MA.** Signaling mechanisms underlying the vascular myogenic response. *Physiol Rev* 79: 387–423, 1999.
8. **Davis MJ, Wu X, Nurkiewicz TR, Kawasaki J, Davis GE, Hill MA, Meininger GA.** Integrins and mechanotransduction of the vascular myogenic response. *Am J Physiol Heart Circ Physiol* 280: H1427–H1433, 2001.
9. **Dong L, Zheng YM, Van Riper D, Rathore R, Liu QH, Singer HA, Wang YX.** Functional and molecular evidence for impairment of calcium-activated potassium channels in type-1 diabetic cerebral artery smooth muscle cells. *J Cereb Blood Flow Metab* 28: 377–386, 2008.
10. **Drummond HA, Grifoni SC, Jernigan NL.** A new trick for an old dogma: ENaC proteins as mechanotransducers in vascular smooth muscle. *Physiology (Bethesda)* 23: 23–31, 2008.
11. **Drummond HA, Jernigan NL, Grifoni SC.** Sensing tension: epithelial sodium channel/acid-sensing ion channel proteins in cardiovascular homeostasis. *Hypertension* 51: 1265–1271, 2008.
12. **Du H, Gu G, William CM, Chalfie M.** Extracellular proteins needed for C. elegans mechanosensation. *Neuron* 16: 183–194, 1996.
13. **Earley S, Waldron BJ, Brayden JE.** Critical role for transient receptor potential channel TRPM4 in myogenic constriction of cerebral arteries. *Circ Res* 95: 922–929, 2004.
14. **Emtage L, Gu G, Hartwieg E, Chalfie M.** Extracellular proteins organize the mechanosensory channel complex in C. elegans touch receptor neurons. *Neuron* 44: 795–807, 2004.
15. **Ge Y, Gannon KP, Gousset M, Liu R, Murphey B, Drummond HA.** Impaired myogenic constriction of the renal afferent arteriole in a mouse model of reduced βENaC expression. *Am J Physiol Renal Physiol* 302: F1486–F1493, 2012.
16. **Geary GG, Krause DN, Duckles SP.** Estrogen reduces myogenic tone through a nitric oxide-dependent mechanism in rat cerebral arteries. *Am J Physiol Heart Circ Physiol* 275: H292–H300, 1998.
17. **Geffeney SL, Cueva JG, Glauser DA, Doll JC, Lee TH, Montoya M, Karania S, Garakani AM, Pruitt BL, Goodman MB.** DEG/ENaC but not TRP channels are the major mechanoelectrical transduction channels in a C. elegans nociceptor. *Neuron* 71: 845–857, 2011.
18. **Grifoni SC, Chiposi R, McKey SE, Ryan MJ, Drummond HA.** Altered whole kidney blood flow autoregulation in a mouse model of reduced β-ENaC. *Am J Physiol Renal Physiol* 298: F285–F292, 2010.
19. **Hill MA, Davis MJ, Meininger GA, Potocnik SJ, Murphy TV.** Arteriolar myogenic signalling mechanisms: Implications for local vascular function. *Clin Hemorheol Microcirc* 34: 67–79, 2006.
20. **Hill MA, Yang Y, Ella SR, Davis MJ, Braun AP.** Large conductance, Ca^{2+}-activated K^+ channels (BKCa) and arteriolar myogenic signaling. *FEBS Lett* 584: 2033–2042, 2010.
21. **Hill MA, Zou H, Potocnik SJ, Meininger GA, Davis MJ.** Invited review: arteriolar smooth muscle mechanotransduction: Ca^{2+} signaling pathways underlying myogenic reactivity. *J Appl Physiol* 91: 973–983, 2001.
22. **Jasti J, Furukawa H, Gonzales EB, Gouaux E.** Structure of acid-sensing ion channel 1 at 1.9 A resolution and low pH. *Nature* 449: 316–323, 2007.
23. **Johnson BD, Mather KJ, Wallace JP.** Mechanotransduction of shear in the endothelium: basic studies and clinical implications. *Vasc Med* 16: 365–377, 2011.
24. **Lee J, Ishihara A, Oxford G, Johnson B, Jacobson K.** Regulation of cell movement is mediated by stretch-activated calcium channels. *Nature* 400: 382–386, 1999.
25. **Lewin GR, Moshourab R.** Mechanosensation and pain. *J Neurobiol* 61: 30–44, 2004.
26. **Lin YW, Cheng CM, Leduc PR, Chen CC.** Understanding sensory nerve mechanotransduction through localized elastomeric matrix control. *PLoS One* 4: e4293, 2009.
27. **Liu J, Schrank B, Waterston RH.** Interaction between a putative mechanosensory membrane channel and a collagen. *Science* 273: 361–364, 1996.
28. **Loutzenhiser R, Bidani A, Chilton L.** Renal myogenic response: kinetic attributes and physiological role. *Circ Res* 90: 1316–1324, 2002.
29. **Loutzenhiser R, Griffin KA, Bidani AK.** Systolic blood pressure as the trigger for the renal myogenic response: protective or autoregulatory? *Curr Opin Nephrol Hypertens* 15: 41–49, 2006.

30. **Maji D, Lahiri SK, Das S.** Study of hydrophilicity and stability of chemically modified PDMS surface using piranha and KOH solution. *Surface Interface Analysis* 44: 62–69, 2012.
31. **Martinez-Lemus LA, Crow T, Davis MJ, Meininger GA.** $\alpha_v\beta_3$- and $\alpha_5\beta_1$-integrin blockade inhibits myogenic constriction of skeletal muscle resistance arterioles. *Am J Physiol Heart Circ Physiol* 289: H322–H329, 2005.
32. **Montell C.** The TRP superfamily of cation channels. *Sci STKE* 2005: re3, 2005.
33. **Morita H, Honda A, Inoue R, Ito Y, Abe K, Nelson MT, Brayden JE.** Membrane stretch-induced activation of a TRPM4-like nonselective cation channel in cerebral artery myocytes. *J Pharm Sci* 103: 417–426, 2007.
34. **Morris CE.** Voltage-gated channel mechanosensitivity: fact or friction? *Front Physiol* 2: 25, 2011.
35. **Pradervand S, Barker PM, Wang Q, Ernst SA, Beermann F, Grubb BR, Burnier M, Schmidt A, Bindels RJ, Gatzy JT, Rossier BC, Hummler E.** Salt restriction induces pseudohypoaldosteronism type 1 in mice expressing low levels of the beta-subunit of the amiloride-sensitive epithelial sodium channel. *Proc Natl Acad Sci USA* 96: 1732–1737, 1999.
36. **Seagard JL, van Brederode JF, Dean C, Hopp FA, Gallenberg LA, Kampine JP.** Firing characteristics of single-fiber carotid sinus baroreceptors. *Circ Res* 66: 1499–1509, 1990.
37. **Setoguchi M, Ohya Y, Abe I, Fujishima M.** Stretch-activated whole cell currents in smooth muscle cells from mesenteric resistance artery of guinea-pig. *J Physiol* 501: 343–353, 1997.
38. **Sharif-Naeini R, Folgering JH, Bichet D, Duprat F, Lauritzen I, Arhatte M, Jodar M, Dedman A, Chatelain FC, Schulte U, Retailleau K, Loufrani L, Patel A, Sachs F, Delmas P, Peters DJ, Honore E.** Polycystin-1 and -2 dosage regulates pressure sensing. *Cell* 139: 587–596, 2009.
39. **Stockand JD, Staruschenko A, Pochynyuk O, Booth RE, Silverthorn DU.** Insight toward epithelial Na^+ channel mechanism revealed by the acid-sensing ion channel 1 structure. *IUBMB Life* 60: 620–628, 2008.
40. **Syntichaki P, Tavernarakis N.** Genetic models of mechanotransduction: the nematode Caenorhabditis elegans. *Physiol Rev* 84: 1097–1153, 2004.
41. **Van Dokkum RP, Alonso-Galicia M, Provoost AP, Jacob HJ, Roman RJ.** Impaired autoregulation of renal blood flow in the fawn-hooded rat. *Am J Physiol Regul Integr Comp Physiol* 276: R189–R196, 1999.
42. **van Dokkum RP, Sun CW, Provoost AP, Jacob HJ, Roman RJ.** Altered renal hemodynamics and impaired myogenic responses in the fawn-hooded rat. *Am J Physiol Regul Integr Comp Physiol* 276: R855–R863, 1999.
43. **VanLandingham LG, Gannon KP, Drummond HA.** Pressure-induced constriction is inhibited in a mouse model of reduced βENaC. *Am J Physiol Regul Integr Comp Physiol* 297: R723–R728, 2009.
44. **Welsh DG, Morielli AD, Nelson MT, Brayden JE.** Transient receptor potential channels regulate myogenic tone of resistance arteries. *Circ Res* 90: 248–250, 2002.
45. **Zeller PJ, Skalak TC.** Contribution of individual structural components in determining the zero-stress state in small arteries. *J Vasc Res* 35: 8–17, 1998.